

Multi-destination Pedestrian Flows in Equilibrium: a Cellular Automaton Based Approach

Luca Crociani

CSAI - Complex Systems & Artificial Intelligence Research Center, University of Milano-Bicocca, Milano, Italy

&

Gregor Lämmel*

Institute for Advanced Simulation, Forschungszentrum Jülich, Jülich, Germany

Abstract: *This article presents a new simulation approach for multi-destination pedestrian crowds in complex environments. The work covers two major topics. In the first part, a novel cellular automaton (CA) model is proposed. The model describes the pedestrian movement by a set of simple rules and produces fundamental diagrams similar to those derived from laboratory experiments. The second topic of this work describes how the CA can be integrated into an iterative learning cycle where the individual pedestrian can adapt travel plans based on experiences from previous iterations. Depending on the setup, the overall travel behavior moves either towards a Nash equilibrium or the system optimum. The functional interaction of the CA with the iterative learning approach is demonstrated on a set of transport paradoxes. Furthermore, time series of speed and density observed in a small-scale experiment show a general agreement between the CA simulation and laboratory experiments. The scalability of the proposed approach is demonstrated on a large-scale scenario.*

1 INTRODUCTION

Research on pedestrian dynamics has grown significantly in the last years due to the increasing need to analyze the safety of public spaces and other pedestrian environments. The global process of urbanization introduced, in fact, new issues in different fields, including transportation, where a growing demand has to be considered at the road level as well as at the pedestrian environment level.

Computer simulations can help identify critical situations which emerge from the complex dynamics of pedestrian crowds. Thus, computer simulations of pedestrian crowds can contribute to the safety of pedestrians on the one hand

and help to optimize the performances of pedestrian environments on the other.

The present work discusses a novel cellular automaton (CA) approach for omnidirectional pedestrian flows in combination with methods for pedestrian wayfinding in complex environments. Following Hoogendoorn and Bovy (2004a)¹, the pedestrian behavior is modeled at three different levels:

- **Strategic level:** the person formulates his/her plan and final objective;
- **Tactical level:** the set of activities to complete the plan is computed and scheduled;
- **Operational level:** each activity is physically executed, e.g., the person walks from one point in the environment to another one.

Within this scope there exists a large body of related works.

1.1 Modeling of Operational Pedestrian Behavior

A large part of the literature focuses on the operational level of pedestrian behavior, where the consistent—but not complete—knowledge about density and flow relation allows the validation of dynamics generated by the models. Macroscopic approaches model pedestrians by abstracting the concept of individuals and considering the crowd as a kinetic gas (Henderson, 1971) or a fluid (Helbing, 1998). Methods taken from continuum mechanics have been proposed as early as 2002 (see, e.g., Hughes, 2002) and applied by numerous works. Xiong et al. (2011) proposed a high-order scheme to numerically simulate the mathematical model of Jiang et al. (2009). The computational complexity of macroscopic models is determined rather by the area of

¹ The same classification has also been provided for vehicular traffic modeling by Michon (1985).

the environment than by the number of people. Thus, macroscopic approaches are efficient for the simulation of large crowds in small spaces. However, the equations generating the dynamics are abstract, making a mapping to an inherent pedestrian behavior difficult.

In contrast, microscopic approaches are built from the individual's point of view. The complex dynamics of microscopic models stem from the interaction between individuals and the interaction of individuals with the environment.

Some microscopic models treat space as a continuous entity. A well-known approach is the force-based model by Helbing and Molnár (1995), where attractive or repulsive forces generate the pedestrian movement. Since then, many alternative formulations have been proposed. Chraïbi et al. (2010) provide a model that uses ellipses to present the velocity-dependent space occupation of pedestrians. Von Sivers and Köster (2014) introduce stride length adaptation to improve the simulated dynamics. Sun and Wu (2014) provide a library of various behaviors with different functions for the operational level of pedestrians.

In alternative to the continuous space approach, CA based models discretize space into a grid-like structure, gaining efficiency in computational times. Historically, CAs have first been applied to vehicular traffic. Nagel and Schreckenberg (1992) introduce a CA model for single lane vehicular traffic, which yields plausible flow dynamics. Rickert et al. (1996) extend this work into a two-lane model that introduces rules for overtaking. Nagel et al. (1998) give a more general approach to simulate two-lane streets, evaluating different rules for managing the overtaking. Simon and Gutowitz (1998) extend this model to bidirectional flows. Moussa (2008) proposes an advancement that prevents passing vehicles from colliding with oncoming traffic. The application of CAs in the field of pedestrian dynamics started with the work of Blue and Adler (1998). In their model, pedestrians are walking on a multi-lane ring road. Pedestrians differ by their desired speed and are capable of performing lane changes. Fukui and Ishibashi (1999) propose a CA model for bidirectional flows, where conflicts with oncoming pedestrians are solved by sidestepping. At low densities the model displays lane formation behavior, but when densities exceed a certain threshold, a rapid state transition from free flow to total jam is observed. Similar state transitions occur in the CA model proposed by Baek et al. (2009). Other works (Muramatsu et al., 1999; Muramatsu and Nagatani, 2000) identify a stable critical density for large systems. Enabling pedestrians to swap positions under dense conditions can avoid the implausibly rapid state transition from free flow to total jam. Blue and Adler (2000a) present a corresponding model for bidirectional flows with *ad hoc* rules. The rules take different desired speeds of pedestrians into account, allowing lane changes and also position swapping in dense conditions, to avoid the freezing of the pedestrian flow. Blue and Adler (2000b)

present a four-directional extension, where the swapping procedure is modeled by a simple probabilistic approach. Whenever two pedestrians are in a head-on conflict, they swap position with a certain probability. Flötteröd and Lämmel (2015) introduced the concept of a conflict delay that pedestrians experience when they swap positions. The density-dependent conflict parameter is fitted against empirical data. Lämmel and Flötteröd (2015) discuss an event-based CA that implements the concept of conflict delay for one-dimensional movement in an isolated channel.

A bio-inspired mechanism is the well-known floor field model by Burstedde et al. (2001). A static floor field increases the probability of movement towards a certain destination, while a dynamic one reproduces the chemotaxis phenomenon, leading to lane formation in simulations of bidirectional flows. Kirchner et al. (2003) extend that model by introducing friction. Kirchner et al. (2004) discuss methods to deal with different speeds, in addition to the usage of a finer grid discretization. An alternative approach to represent different speeds in a discrete space is given by Bandini et al. (2015).

1.2 Route Finding and Equilibrium Search at a Strategic and Tactical Level

In real life situations—for example in large train stations—individual pedestrians have distinctive origins and destinations. At the strategic level pedestrians plan their ultimate destinations. At the tactical level they plan and schedule activities or intermediate targets that lead to the desired destination. The schedule of intermediate targets describes a route from the origin to the destination. Early works in transportation research consider the so-called shortest path solution (SP) as an adequate route assignment (see, e.g., Whiting and Hillier (1960)).

A drawback of SP is that it does not consider congestion. Consequently, resulting travel times can be longer than expected. This is in particular a problem for evacuations, where the available safe egress time is limited (see, e.g., Lämmel et al. (2010)). When traveling, people usually try to minimize travel time, thus, the SP seems to assign unrealistic routes also in behavioral terms.

An assignment of routes where individual travel times are minimal under the given circumstances is called dynamic user equilibrium or Nash equilibrium (NE). It describes a state in a competitive game where no player can gain by unilaterally switching his/her current strategy (Nash, 1951). It corresponds to Wardrop's first principle for road traffic, which states that at equilibrium, the journey times of all routes that are actually used are equal or less than those that would be experienced on any unused route (Wardrop, 1952). An NE can be achieved by iteratively assigning travelers new routes which are best responses to the situation in the current iteration. If at any time the best responses do not lead to new route assignments, the system has converged to an NE. A detailed discussion on the application of

iterative best-response strategies to transport route assignment problems is given in Cascetta (1989). Gawron (1998) proposes a simulation-based iterative algorithm where the travelers try to minimize their experienced individual travel times. The performance of the proposed algorithm is demonstrated on the so-called Braess's paradox (Braess, 1968). Nagel et al. (2000) present an application in a large-scale context. Raney and Nagel (2004) discuss a method that aggregates the experienced travel times over predetermined time slices for faster computation. Since an aggregation of experienced travel times may introduce a bias by systematically over- or underestimating the actual travel time, Raney and Nagel (2004) introduce an agent database that keeps a certain number of routes in the individual agent's memory for later execution. At each iteration, agents may either create new best-response routes or select from their memory. Good results in terms of fast relaxation have been achieved by using a Metropolis sampling like (Metropolis et al., 1953) selection mechanism.

Hoogendoorn and Bovy (2004a) propose a macroscopic continuous time and space dynamic iterative assignment model based on a generalized cost function. The generalized cost function aggregates over a range of different cost contributors such as travel time or penalties for late arrivals. While the original model deals with inelastic demand (all travelers starting at once), the authors argue that a generalization to a framework based on activity-chains would be straightforward (Hoogendoorn and Bovy, 2004b). An activity chain is a decomposition of a traveler's routines. A similar approach for the optimization of all-day, activity chain-based plans is discussed in Charypar and Nagel (2005).

An application of the theory on NE to the exit door selection problem in evacuations is discussed in Ehtamo et al. (2010). Lämmel et al. (2009) discuss the application of NE in the context of large-scale pedestrian evacuation problems. On a similar but smaller scale, Kretz et al. (2014) discuss NE assignments for pedestrians under normal conditions. A static NE assignment method is discussed in Bauer and Gantner (2014).

As an NE minimizes individual travel times, it does not necessarily minimize the system travel time (i.e. the sum of all travel times). A state where the system travel time is minimal is called system optimum (SO). Interestingly, the SO corresponds to an NE with respect to the marginal social costs instead of travel times (Beckmann et al., 1956). For an individual traveler, the marginal social costs comprise his/her experienced travel time and the amount of time that he/she delays other travelers. Peeta and Mahmassani (1995) propose an iterative algorithm in the dynamic traffic assignment domain. Lämmel and Flötteröd (2009) discuss a multi-agent-based approach with deterministic travel times that relies on a simple approximation to estimate the marginal social costs. A comparison with a numerical solution for a large-scale pedestrian evacuation scenario shows that the proposed approximation gives reasonable results

(Dressler et al., 2011). Similarly, the work of Hamacher et al. (2011) uses numerical solutions in order to determine lower evacuation time bounds.

A metaheuristic approach to find optimal distributions of routes—in terms of shortest evacuation times by also considering road conditions—is the one by Forcael et al. (2014). The model employs an ant colony optimization algorithm to find optimal evacuation routes in a city area by assuming evacuation on foot.

Kemloh Wagoum et al. (2012) propose dynamic route planning procedures where initial routes are adapted as the local situation changes. Other works on pedestrian route finding include (Asano et al., 2010; Guo and Huang, 2011).

1.3 Empirical data of omnidirectional pedestrian flows

AlGadhi et al. (2002) identify a considerable bidirectional flow even for high densities of up to 7 pers/m² during a pilgrimage. Helbing et al. (2005); Kretz et al. (2006) present laboratory experiments on bidirectional flows of various flow compositions. They find that for high densities, the sum of directional flows in the bidirectional case is higher than in the unidirectional case.

Zhang et al. (2012) derive uni- and bidirectional fundamental diagrams (FD) from laboratory experiments. The unidirectional FD display the typical triangular shape with a single peak flow at medium densities, while the bidirectional FD ends in a plateau with a considerably higher flow compared to the unidirectional one. Liu et al. (2014) present similar findings.

Plaue et al. (2011, 2012) investigate pedestrian streams in a 90- and a 180-degree crossing experiment. The observed flow-density relation for both experiments fits well with the bidirectional FD of Zhang et al. (2012) (Zhang and Seyfried, 2014).

1.4 Synthesis

Approaches to model the operational level of pedestrian movement can be categorized into three classes. (i) Macroscopic approaches that consider the crowd as a kinetic gas or fluid. Those approaches are computationally efficient for large crowds in small spaces. However, the negligence of the individual makes it impossible to track persons and difficult at least to model complex multi-destination pedestrian crowds. (ii) Force-based models simulate pedestrians as individuals. However, the computational cost of those models makes them unpractical for large scenarios. (iii) CAs are both microscopic and computationally efficient. CAs are capable of reproducing aggregated features like lane formation in bidirectional flows. Still, at high densities, existing models display unrealistic jamming (e.g. Baek et al, 2009) or deal only with one-dimensional streams (Lämmel and Flötteröd, 2015).

In contrast to the operational level, research on the tactical and strategic level is limited. Existing models are either macroscopic (Hoogendoorn and Bovy, 2004a), geared to-

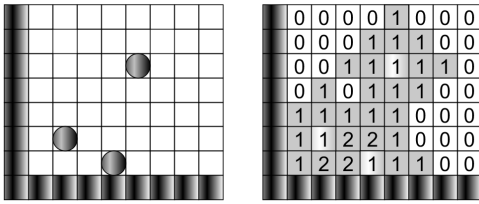


Figure 3. The *density grid* working principle: at the beginning of the time-step, pedestrians signal their presence by adding 1 in the nearby cells (here the radius is 2 cells).

approach has been introduced in Burstedde et al. (2001). A relevant aspect is the way in which gradients are diffused from the targets. Different spreading methods can lead to different space utilizations of the simulated pedestrians. The work of Kretz et al. (2010) gives an overview about the most common methods. Figure 2 illustrates the *Manhattan* metric and the *Chessboard* metric with the $\sqrt{2}$ variant over corners. This work applies the *Chessboard* metric.

An important aspect of the floor field diffusion algorithm is the stopping criterion. If no stopping criterion is defined, the floor field is spread to all cells of the environment. In this work, the diffusion stops at obstacles and (intermediate) targets. The main reason for stopping at (intermediate) targets is to allow a complete representation of all possible paths, as shown in Figure 1. In general, it allows to map the environment onto a network where nodes represent targets and links describe a direct connection between two targets (i.e. there are no other intermediate targets to cross in between). This makes path computation simple and reduces the computational costs, because floor fields are only computed where needed. Moreover, it allows parallelizing the floor field computation in a simple way. The resulting network is used on the tactical level for route computation. Details are discussed in Section 3.

2.2 The Local Density Estimation

The proposed CA model reproduces empirically derived fundamental diagrams as well as disaggregated dynamic situations. A simple set of rules controls the CA model. Those rules depend on the local density. A feasible density estimation approach is therefore needed. Several methods have been defined in the literature (cf., Steffen and Seyfried (2010)). A versatile method is the so-called *Voronoi* method. It provides stable and continuous values for the local densities, without the need of any calibration parameter. However, its computational complexity is considerable and in the case of discrete models its improvements in precision are limited. The computational cost of this model has been kept low by introducing a more simple and efficient method, which performs a discrete calculation of the local density to achieve the *number density* of pedestrians. This quantity describes the overall density of people in the surrounding of each cell within a constant distance.

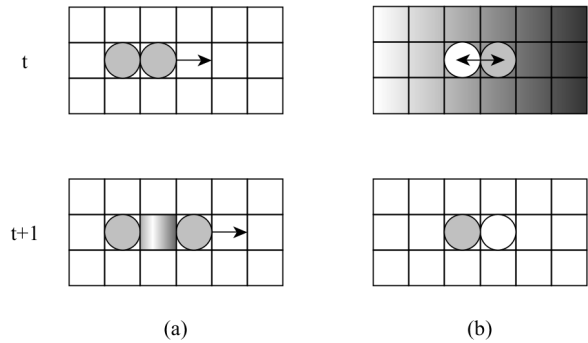


Figure 4 The *jam* (a) and *counter-flow* (b) rules. In (a), the cell that became empty remains blocked. In (b) two counter-flow pedestrians (the light pedestrian follows the dark color and vice-versa) swap their positions.

This estimation is calculated with an additional grid that works as a dynamic floor field and changes its values over time. The idea is to spread the presence of each pedestrian to the surrounding space, i.e., to cells belonging to a fixed distance d . This parameter defines the local aspect of the density calculation and is the only parameter of this method. The local density ρ of cell c is defined as

$$\rho = \frac{n}{A(c)}, \quad (1)$$

with n representing the number of persons within the distance d from the center of the cell c and $A(c)$ is the area of the set of cells that (i) belong to the same neighborhood and (ii) do not contain obstacles. The latter enforces that obstacles are not part of the local area.

The update phase of the density grid is illustrated in Figure 3: at the beginning of each simulation step, the presence of pedestrians is spread to the surrounding cells which are not containing obstacles within radius d . In this way, each cell of the grid contains the n value. The area $A(c)$ must be calculated for every cell of the environment at the beginning of the simulation, but in any case the total cost of the computation grows linearly with the number of pedestrians (see Section 4.4 for an analysis of the computation times).

The discussed method leads the density estimation to be isotropic. However, it is well known that pedestrians perceive their surroundings in an anisotropic way (see, e.g., Gulikers et al. (2013)). In the proposed CA model the anisotropy is thus implemented by the update rules as discussed in the following section.

2.3 Rules of the Dynamics: Definition and Implementation for Two-dimensional Environments

The proposed CA model offers a computationally efficient calculation of the pedestrian dynamics in two-dimensional environments. Table 1 gives a parameter overview. It extends the ideas of Flötteröd and Lämmel (2015), who discuss a theoretical model on one-dimensional pedestrian flows. In the theoretical model, the movement is controlled by three rules.

Table 1

Parameter overview of the CA model	
<i>Parameter</i>	<i>Value</i>
density spreading parameter d	2
time-step duration τ_m	0.3s
conflict delay coefficient β	0.39s
conflict delay exponent γ	1.43
normalization factor η	1
sensitivity parameter κ_F	6
cell side length $cell_side$	0.4m

- **Movement rule:** a pedestrian cannot change his/her position before τ_m seconds,

- **Jam rule:** if a cell is occupied at time t by pedestrian p , every pedestrian $\bar{p} \neq p$ cannot occupy that cell before time $t + \tau_j$,

- **Counter-flow rule:** if two pedestrians in two neighboring cells at time t are in a head-on conflict, then they will swap their position ("squeeze past" each other) at time $t + \tau_s + \tau_m$.

The movement rule defines the free-flow cell travel time, as well as the *time-step* duration of the CA. In this way the equal maximum speed for all pedestrians is given by the ratio $cell_side/\tau_m$. In the present work, τ_m is assumed to be 0.3s in order to have a pedestrian speed of about 1.3 m/s. Other approaches allow for individual maximal speeds. Kirchner et al. (2004) propose a model with a discrete number of individual speeds. Bandini et al. (2015) discuss a model where the movement is controlled by probabilities and thus can reproduce a continuum of expected maximal speeds. These approaches allow to overcome artifacts resulting from the space discretization, as well as from the diagonal movements that here imply an increase of the pedestrian speed by $\sqrt{2}$. This contribution focuses on the reproduction of fundamental properties, in particular for higher densities. Therefore individual maximal speeds are out of scope, but will be part of future directions.

Flötteröd and Lämmel (2015) discuss the following continuity constraint, without which the model would behave discontinuously when going from arbitrary small but strictly positive counter-flow to a unidirectional flow.

$$\tau_j = \tau_m + \tau_s \quad (2)$$

Furthermore, they make the jam and counter-flow parameters density dependent and use a least squares estimator to fit the model against empirical data. The density dependence is defined by the following equation:

$$\tau_s = \beta \left(\frac{cell_side \cdot \rho}{m-1} \right)^\gamma, \quad (3)$$

where $cell_side$ is the width of the pedestrian, ρ is the local

density for the pedestrian under consideration, and (β, γ) are parameters.

This contribution extends the work of Flötteröd and Lämmel (2015) and the related computer implementation of Lämmel and Flötteröd (2015) to two-dimensional environments. In a one-dimensional environment, the movement is constrained to streams of pedestrians, while in a two-dimensional environment pedestrians can move freely in multiple directions. There are various options for modeling the direction choices.

In this work, pedestrians choose their movement directions by a simple probability function, similar to the one provided by Burstedde et al. (2001). The movement capabilities of pedestrians are restricted to the Moore neighborhood, allowing them to also perform diagonal movements. The probability for a pedestrian at location xy to move to the cell with coordinates ij is:

$$P_{ij} = \eta \epsilon_{ij} e^{\kappa_F (F_{xy} - F_{ij})} (1 - \Omega_{ij}), \quad (4)$$

where η is a normalization factor; ϵ_{ij} describes the impenetrability of obstacles (i.e. 0 if there is an obstacle in ij , otherwise 1); F_{xy} and F_{ij} are the values of the static floor field respectively for the position of the pedestrian and the evaluated position³; Ω_{ij} forbids movement to cells already occupied by other pedestrians by returning 1 if ij is not free or 0 otherwise; κ_F is a calibration parameter.

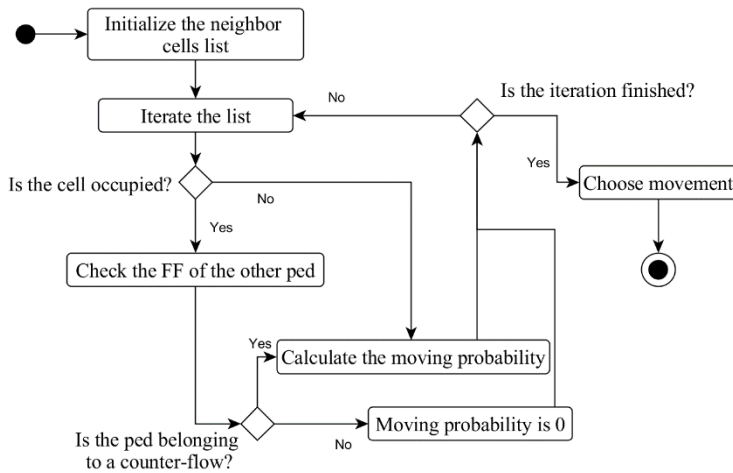
The *update strategy* is parallel, which means that not all movement intentions lead to a position change at the end of the step. Conflicts arising from choices of identical destinations are dealt with by randomly choosing a winner, leaving the other involved pedestrians to yield and choose a new move at the next simulation time-step.

The adaptation and implementation of the jam and counter-flow rules are graphically explained in Figure 4.

The first mechanism implements the jam rule by extending the presence of pedestrians for τ_j time to their previously occupied cells. The procedure works as follows: each pedestrian who moves at time t leaves a tag ω_t on his/her previous position. This tag will act as an obstacle for every person until time $t + \tau_j$. In this way, every person will cause a delay only to the persons behind. Thus the leaders of a line will not be affected by the eventual congestion behind them and, albeit density perception is isotropic, the overall behavior is anisotropic, as observed in real life. Since time is discrete, a naïve implementation of this mechanism would require τ_j to be a multiple of the *time-step* duration τ_m . Nonetheless, a usage of $\tau_j \in \mathbb{R}$ is allowed and has been implemented by introducing a stochastic management of this variable. The tag ω_t stays in the cell for at least $\lceil \tau_j / \tau_m \rceil$ simulation time-steps, while the decimal part of the

³ This represents a difference to the original model of Burstedde et al. (2001), in order to let the value of the exponent to be normalized in a defined range.

Pedestrian - Choice of Movement



Pedestrian Synchronizer - Check of Swapping

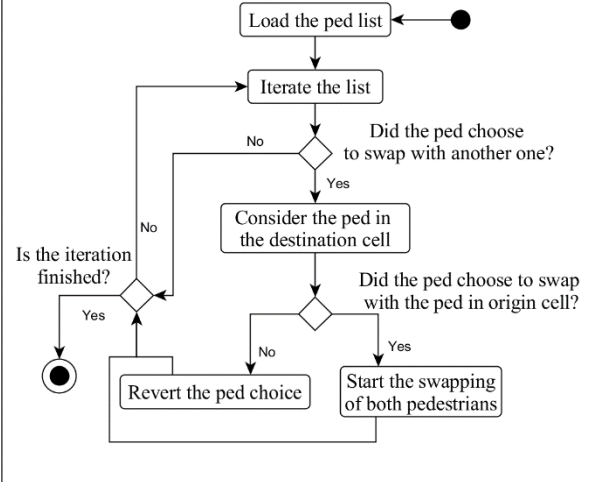


Figure 5 Activity diagram illustrating the swapping rule of the CA. Pedestrians check the direction of the others in front by the floor field (FF) and are allowed to choose movements to positions occupied by counterflow pedestrians. At the end of the step, the *Pedestrian Synchronizer* swaps only those pedestrians whose movement choices match.

fraction defines the probability that the trace stays for one additional time-step longer. This aspect is important since the τ_j varies with the local density ρ , according to the continuity constraint (2) and the density dependent conflict delay (3).

The counter-flow rule implies that two pedestrians who choose to swap their position, due to opposite movement directions, will do so after $\tau_m + \tau_s$ seconds. The question of having $\tau_s \in \mathbb{R}$ is again valid as discussed above, and an analogous method is used.

A deeper clarification of the definition and recognition of counter-flow during the simulation is necessary, when the position swapping becomes available for the two pedestrians, and how it is performed (see Figure 4(b) for illustration). The swapping, in fact, is a coordinated action, which needs to be synchronized. To allow this, the algorithm graphically explained in Figure 5 has been introduced, designing the following *hand-shaking* protocol: (i) pedestrian p chooses to move to the cell where pedestrian p' resides; (ii) pedestrian p' chooses to move to the cell of pedestrian p ; (iii) pedestrian p and p' swap positions and start waiting $\tau_m + \tau_s$ seconds before they choose the next move.

This sequence of events describes only the successful option: if one of the two pedestrians does not choose to swap, the other one will stay where he/she is and choose a new move in the next simulation time-step. In any case, the *hand-shaking* protocol starts with the assumption that at least one of the two pedestrians chooses to move to the position of the other. The probability function (4) would not allow this kind of selection due to Ω_{ij} . To solve this issue, Ω_{ij} needs to return 0 not only for empty cells, but also for those that are occupied by *counter-flow pedestrians*.

Counter-flow pedestrians can be identified by comparing values of the individual perceived floor fields. Assuming pedestrian p and p' are at locations ij and xy respectively, with each cell belonging to the Moore neighborhood of the other, pedestrian p will identify p' as a *counter-flow pedestrian*, and vice versa, if and only if both values $F_{ij} - F_{xy}$, by considering the static floor field felt by p' , and $F_{xy} - F_{ij}$, by considering the static floor field of p , are positive, i.e., they effectively belong to two opposite flows.

2.4 Validation of the Operational Level

To validate the CA on the operational level, a unidirectional and a bidirectional experiment have been performed. The settings mimic those of the laboratory experiments of Zhang et al. (2011) and Zhang et al. (2012). Thus, a straightforward comparison of the simulation results with the empirical observations is possible. The comparison is limited to the unidirectional and bidirectional FD. In the experiments, the pedestrians walk through a channel. For the unidirectional case, the inflow into the channel is controlled by an entrance bottleneck, while the outflow is limited by an exit bottleneck of variable width. For the bidirectional case, entrance bottlenecks just in front of the channel control the inflows. The outflow is unbounded, which means pedestrians can leave the channel unhindered either to the right or to the left, circumventing the entrance bottlenecks. In the bidirectional case, the flows are balanced (i.e. inflow and consequently directional densities are similar). To cover the whole range of densities, a number of simulations with variable population sizes have been set up.

To determine the flow generated by the CA, the travel time from the beginning to the end of the corridor has been recorded for every pedestrian, converting it to the specific

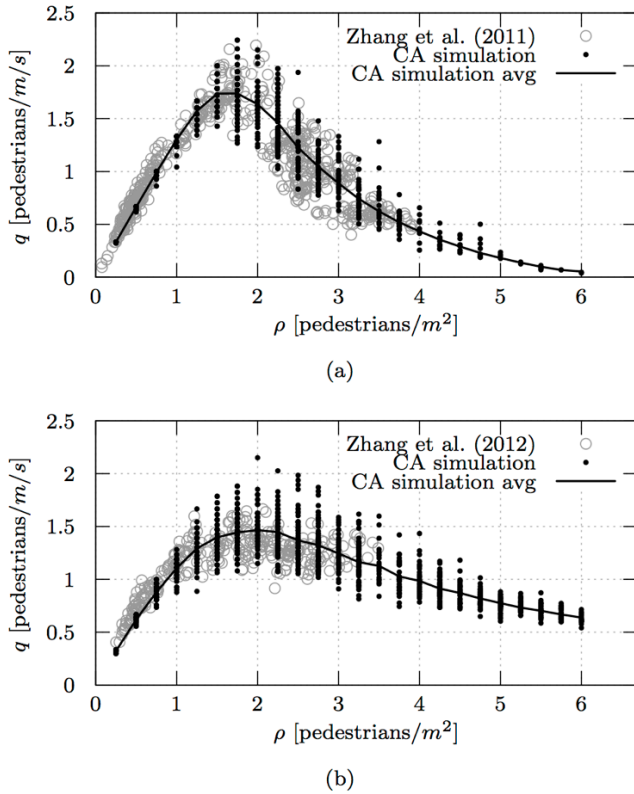


Figure 6 FDs for unidirectional (a) and bidirectional (b) flows. Black dots are measurements from the simulations, while gray circles are the empirical data from Zhang et al. (2011, 2012). Average flow per simulated density is indicated by the solid curve.

flow according to $J(\rho) = \rho \cdot v$, where $v = \text{corridor_length}/\text{travel_time}$ describes the average speed of the simulated pedestrians and ρ the average density inside the channel. For every setting, the simulation has been run long enough with a sufficient number of pedestrians to reach stationarity (i.e. until flow and density remain constant). For both uni- and bidirectional case, the simulation-based FD is created from measurements that are collected during stationary states.

A comparison of simulation-based FDs with those of the laboratory experiments is given in Figure 6(a) and 6(b). Simulation-based results show an almost perfect agreement with the available empirical data. Nevertheless, the simulation extrapolates to densities for which no empirical data exists.

The plot for the bidirectional case in Figure 6(a) demonstrates that the model is able to sustain stable flows over the whole density range and thus overcome the implausibly rapid state transition from free flow to total jam as observed, e.g., in Fukui and Ishibashi (1999) and by Baek et al. (2009). Another observation is that for high densities beyond capacity, the bidirectional flow exceeds the unidirectional flow. This is in line with findings that have been widely reported in empirical studies (see, AlGadhi et al.,

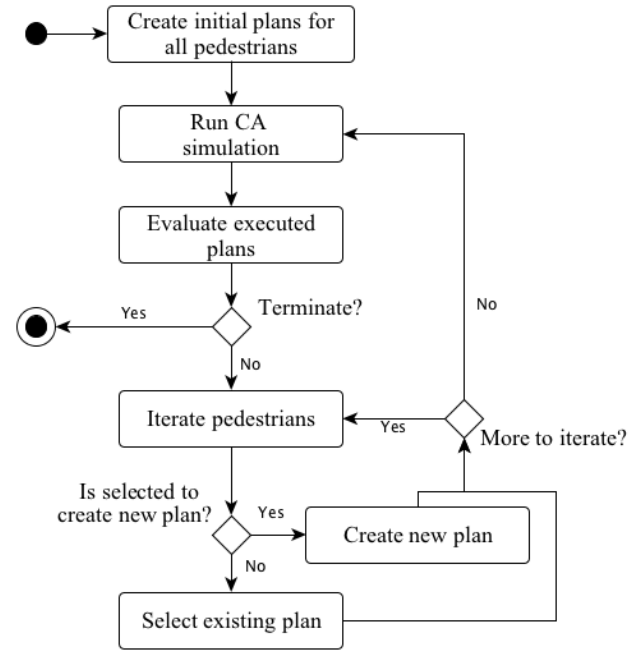


Figure 7 Illustration of the route assignment search strategy.

2002; Helbing et al., 2005; Kretz et al., 2006; Zhang et al., 2012; Liu et al., 2014).

3 ROUTE ASSIGNMENT SEARCH STRATEGY

This section discusses the route assignment on the strategic and tactical level. Raney and Nagel (2004) propose an iterative approach, where vehicular route assignments move towards a Nash equilibrium (NE). Oncoming vehicles move in opposite lanes and thus do not interact. In contrast, this contribution deals with a CA simulation for omnidirectional pedestrian flows. Besides the question of general applicability, this also raises some computational issues.

The general approach is depicted in Figure 7. At startup, the simulation framework creates initial plans. In the underlying work, plans are limited to routes with specific departure times⁴. The initial plans are executed in the CA simulation and subsequently evaluated. After the plans evaluation it must be decided whether to continue or to terminate. If the simulation framework runs on, the pedestrians will revise their travel plans before the cycle starts again. Subsequently, Section 3.1 discusses plans creation, Section 3.2 plans selection, and Section 3.3 the termination criterion.

⁴ In general, plans can cover complex activity chains, e.g. of travel related daily routines. This is, however, beyond the scope of this contribution.

3.1 Plans creation

As discussed in Section 2.1, the simulation environment is mapped onto a set of nodes (targets) that are connected by unidirectional links. Routes (i.e. lists of targets) for the initial plans are computed by the A^* shortest path algorithm. Link weights correspond to free speed travel times. The free speed travel time T_a^{free} for link a of length l_a is defined as:

$$T_a^{free} = \frac{l_a \tau_m}{cell_size} \quad (5)$$

The actual length of a link is not obvious, since a link represents a rather abstract relation from one target (origin) to the next target (destination). A reasonable behavioral assumption is that, in the absence of others, real people choose the shortest connection between two targets. The length of the shortest connection from an origin to a destination has implicitly already been computed by the floor field generation (see Section 2.1). The value of the floor field for a given cell corresponds to the shortest distance between this cell and the origin from where the floor field has been spread. In this way, link lengths are determined at the startup of the simulation.

When pedestrians travel from one target to the next, they experience individual travel costs. Travel costs are averaged over time slices k and stored in hash tables for later use as discussed in (Lämmel et al., 2010). An obvious travel cost component is travel time.

Pedestrians who are selected to create a new plan compute new routes based on the averaged time-dependent travel costs from the previous CA simulation run.

Let $T_a(k)$ denote the averaged time-dependent link travel time of link a and time slice k . If time is the only travel cost component, then the overall route assignment moves towards an NE.

Another component is the time-dependent delay that individual pedestrians impose on others because of their route choice. Following the nomenclature used in economics, the time-dependent delays imposed on others are external costs, while the time-dependent travel times are internal costs. Let $E_a(k)$ denote the time-dependent external costs that a pedestrian imposes on others if he/she enters link a during time slice k . The sum of internal and external costs yields the marginal social costs:

$$M_a(k) = T_a(k) + E_a(k). \quad (6)$$

If new routes are computed based on the marginal social costs, the overall route assignment moves towards the system optimum (SO). Unlike internal costs (travel times), external costs are not directly observable, but they can be derived from the observed flow dynamics of the CA simulation. Lämmel and Flötteröd (2009) give a continuous formulation of the external costs for a queue simulation model. They derive the following approximation from the continuous formulation:

$$e(t_0) = t^e - (t_0 + T^{free}), \quad (7)$$

where $e(t_0)$ are the individual external costs for a traveler who entered a congested link at time t_0 and t^e is the time

when the congestion dissolves. In the following, a simpler implementation in the CA simulation context is discussed.

External costs occur only on delayed links. These are links where obstruction occurs. The current implementation estimates the external costs for all links isolated and thus neglects spillback. Furthermore, it is assumed that the flow on the isolated links is stationary for the whole period of delays. Assume the pedestrian under consideration enters link a at time t and leaves it again at time t' . The pedestrian traversed link a during a period of delays if and only if $t' - t > T_a^{free}$. In this case, the pedestrian imposed external costs on the system. Under the stationarity assumption, the outflow q_a of link a stays constant for the whole period. Thus, the amount of delay the pedestrian imposes on each subsequently following pedestrian is $1/q_a$. The number of delayed pedestrians is equal to $q_a \cdot (t^e - t')$. This yields for its individual external costs

$$e(t) = q_a \cdot (t^e - t') \cdot \frac{1}{q_a} = t^e - t'. \quad (8)$$

The individual external costs are in the same way aggregated and stored in hash tables as the travel times.

NE routing and SO routing are applied under the assumption that travel costs remain the same from one CA simulation run to the next. However, running the CA simulation with changed route assignments might also change the travel costs. A best practice to deal with this issue is to select only a fraction of 10% of all pedestrians for new plans creation. Those pedestrians who do not create new plans select a previously executed one from their memory.

Section 3.2 Plans selection

The plans selection procedure is similar to the Metropolis sampling approach (Metropolis et al., 1953). In order to apply this approach, plans need to be scored. The score of a plan is the negative value of its experienced travel costs (travel times for NE and marginal social costs for SO). s_c is the score of the currently executed plan and s_r is the score of a randomly selected plan from memory. The probability to switch from the current plan to the randomly selected one is

$$p_{switch} = \min(1, \kappa \cdot e^{\lambda \cdot (s_r - s_c)/2}). \quad (6)$$

The parameter κ reflects the probability to switch when both plans have the same score and λ is a sensitivity parameter. In this work these parameters are set to $(\kappa, \lambda) = (0.01, 1)$.

3.3 Termination criterion

The simulation framework should terminate once the desired route assignments haven been reached (i.e. either NE or SO). This opens two questions; (i) how to detect whether NE or SO have been reached and (ii) does the system converge after all?

The first question can be answered by performing a simple test. An intrinsic property of an NE is that nobody can find a faster route by unilateral re-routing. Furthermore, the

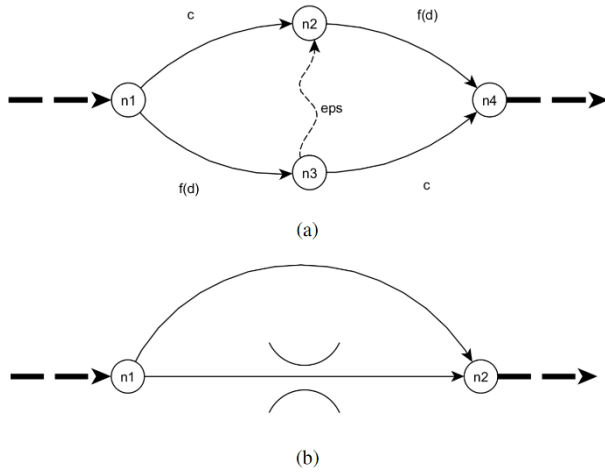


Figure 8 Graph representations of the network explained by Braess (1968) (a) and Daganzo (1998) (b). Labels of edges represent their cost.

SO corresponds to an NE with respect to the marginal costs instead of travel times (Beckmann et al., 1956). Thus, SO and NE can be verified by the same test. An according test would have to iterate over all pedestrians to create new plans. If the new plans are identical to the old ones, the system would have reached a fixed point and thus an NE or the SO, depending on the cost function. This leads to the question of convergence and uniqueness.

Because of the stochasticity of the system, a fixed point might never be reached and convergence and uniqueness remain unclear. Instead, the termination criterion is decided heuristically by looking at the changes in average travel times over iteration cycles. Once those changes remain small, the system is in a relaxed state and the simulation framework terminates.

4 EXPERIMENTS

The overall performance of the proposed simulation framework is demonstrated by a number of computer simulations. Section 4.1 tests the simulation approach on well-known transportation paradoxes. Section 4.2 investigates the reproducibility of laboratory experiments. Scalability and computational performance are demonstrated in Section 4.3.

4.1 Paradoxes in Transportation Networks

The transportation paradox by Braess (1968) is illustrated in Figure 8(a). After an initial long channel, the network presents a choice between two paths, a long one (c) with a constant travel time and a shorter one ($f(d)$), the travel time of which is affected by the number of travelers. Con-

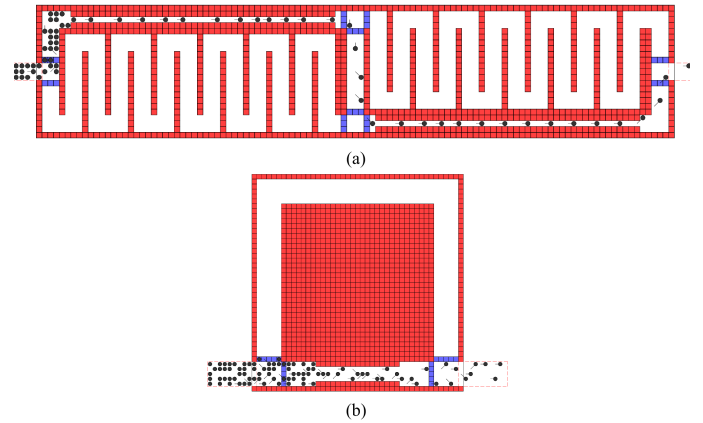
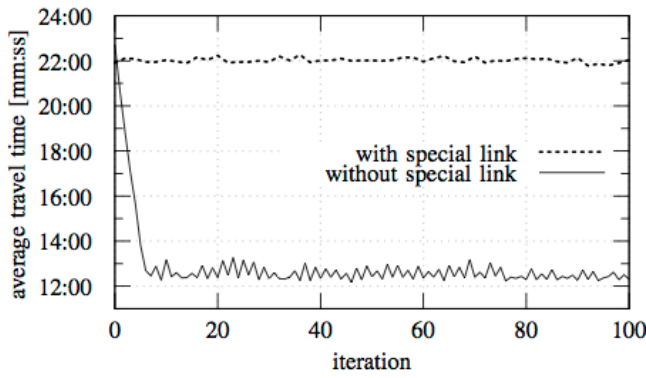


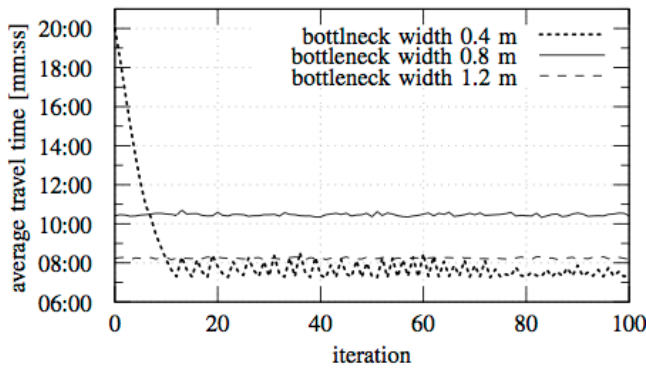
Figure 9 (a) Implementation of the Braess and (b) Daganzo experiments. The environment borders and blue objects represent the nodes of the underlying network.

necting the two nodes at the center, as illustrated by the dashed link, will influence the path choice of the travelers, leading to a decrease of the network performances. The paradox asserts that an improvement to the structure of the network can lead to a worsening of the outgoing flow under Nash conditions, but does not do so for the SO. To simulate the situation defined by the paradox, the pedestrian environment has been configured as in Figure 9(a). The two narrow corridors (top left and bottom right) represent the capacity-restricted short links of the Braess paradox. The high capacity links are modeled as wide zigzag corridors (bottom left and top right). The central corridor implements the special link in the Braess paradox (dashed link in Figure 8(a)). In the absence of the special link, the pedestrians will utilize the upper and the lower path equally. However, once the special link is there, at least a fraction of pedestrians will walk from the top left narrow corridor via the special link to the bottom right narrow corridor. Once this happens, the path via the wide bottom left corridor to the narrow bottom right corridor becomes slower than the analog path along the top. Thus, more and more pedestrians will switch to the top left narrow corridor, leading to a complete disuse of the bottom right wide corridor. Effectively, the capacity of the network will be reduced to that of one single narrow corridor.

A crowd of 2,000 pedestrians walking from the left entrance to the right exit of the environment has been set up. Figure 10(a) shows the results for the NE approach. In case the special link is not present (i.e. the central corridor is blocked by obstacles), the average travel time stabilizes at about 13 minutes. Once the central corridor becomes available, the average travel time increases to 22 minutes. Thus, the NE route assignment behaves exactly as Braess asserts.



(a)



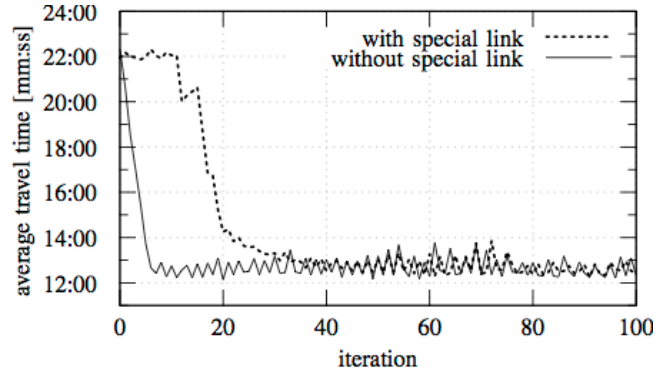
(b)

Figure 10 Average travel times for the simulations of the Braess (a) and Daganzo (b) paradox scenarios.

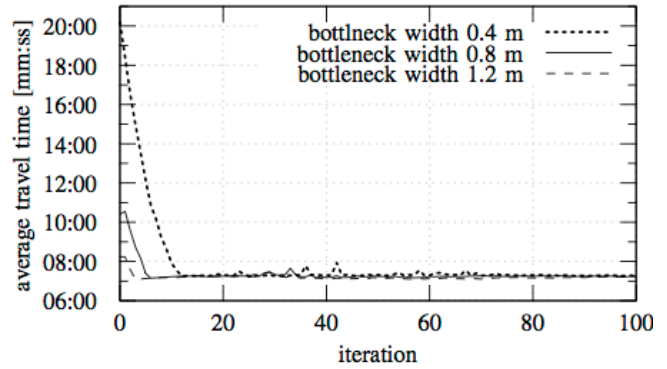
Since the SO is a state with minimum average travel time, the presence of the special link must have no negative impact. As shown in Figure 11(a), where the average travel time is about 13 minutes in both cases, the SO approach works as expected.

Daganzo (1998) discusses a generalization of the Braess paradox, exemplifying another situation where a structural improvement to the network reduces the outflow for NE. The described network is reported in Figure 8(b), characterized by a choice between a short link containing a bottleneck, and a longer but wider one. If the examined network is improved by increasing the width of the bottleneck—until the travel time of the short link is smaller than the other one, even in the congested case—the Nash equilibrium will imply disuse of the long link, negatively impacting the outgoing flow from the network.

To represent this example, the environment for the CA has been designed as in Figure 9(b). Three sets of experiments have been conducted, describing different bottleneck widths inside the short link, with a crowd size and arrival frequency similar to the configuration of the Braess experiments. NE results are shown in Figure 10(b), explaining the key point of the paradox: once a condition of equilibrium is reached, the average travel time related to the scenar-



(a)



(b)

Figure 11 Iterative system optimum search for the scenario of the Braess (a) and Daganzo (b) paradox.

io with the narrowest bottleneck is lower or equal to the other ones. Similar to the Braess example, those paradoxes are not observed in the SO case, as depicted in Figure 11(b).

These observations imply an interesting application of the Nash equilibrium and system optimum approach. It is generally accepted that travelers try to minimize their individual travel time during their daily commutes. Thus, transport systems are rather in a state of an NE than in the state of the SO. However, as it has been shown in the experiments, there might be situations where the SO solution coincides with an NE in a slightly different network. Moreover, the SO also indicates how the network has to be changed in order to force an NE towards the SO. An approach to realize this could make use of the observed flows in the SO and use these values as the maximum allowed flow for an NE (e.g. by introducing artificial bottlenecks). This approach has indeed limitations as it makes the assumption of static flows⁵. Still, it works for both paradoxes

⁵ The static flow assumption can be softened to a piecewise static flow assumption by introducing dynamic bottlenecks that can be adapted over time.

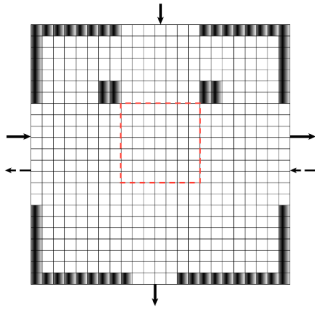


Figure 12 CA grid layout for both 90- and 180-degree intersection experiments.

discussed in this section. In the Braess example, no pedestrian takes the special link in the SO case. This implies that when blocking the special link, the NE coincides with the system optimum (cf. Figs. 10(a) and 11(a)), which is exactly what is stated in (Braess, 1968). For the Daganzo experiments, it is observed that in the SO case the flow on the restricted short link never exceeds the flow that can be handled by a bottleneck of 0.4 m width. Thus, restricting the flow to this value, the NE also moves towards the SO. This has indeed been shown in Figure 10(b). The ratio between the average travel time of an NE and the SO is also known as the *price of anarchy*. It indicates how much gain is possible by changing the layout of the network or the behavior of the travelers (cf., e.g., Roughgarden, (2005); Youn et al., (2008, 2009) for a detailed discussion on this matter).

4.2 Effects of Bidirectional Flows on the System

The proposed model is tested on two data sets gathered at Technical University Berlin in Germany. The first dataset describes a bidirectional flow experiment where two groups of pedestrians move past each other with an intersection angle of 180 degree. The groups consist of 47 and 51 volunteers respectively. Details about the experiments and the data set are discussed in (Plaue et al., 2011).

Plaue et al., 2012 report a dataset of a crossing experiment, where two groups of pedestrians cross at an intersection angle of 90 degrees. The groups consist of 78 and 143 volunteering university students respectively.

The general layout is the same for both experiments. The CA grid layout is depicted in Figure 12. Solid arrows indicate the movement direction for the 90-degree intersection experiment and the solid left-to-right arrows and the dashed arrows indicate the movement directions for the 180-degree intersection experiment.

One way to appraise the feasibility of the proposed simulation model is comparing time series for speed and density resulting from the simulation with those observed in the laboratory experiments. To do so, it is necessary to apply the same method to collect the data for both the simulation and the experiments. Densities and speeds are measured in a 7-by-7 cells area (2.8 m x 2.8 m) as indicated by the dashed red square in Figure 12, using a method based on

Steffen and Seyfried (2010). The CA simulation resolves conflicts probabilistically (see Section 2.3). Thus, speeds, flows and travel times are stochastic and depend on the initial random seed. To appraise this effect, each simulation run has been repeated 1,000 times with different random seeds, and both the time series of average density (speed) and the corresponding standard deviation are reported in the following plots. Figure 13 refers to the 180-degree intersection experiment. It compares the time series of average density (a) and average speed (b). There is a good general agreement between the simulation and the experiments. The standard deviation sd is small, indicating that the dynamics produced by the CA simulation is independent of the random seed. Towards the end (after 27 sec), there is a deviation in the observed speed. While the simulated speed remains constant, the observed speed from experiment drops. One explanation for this deviation is that in the laboratory experiments, the last pedestrians walking through the scene display a lag of motivation and are walking much slower than actually possible⁶. The proposed CA does not model different kinds of motivation but instead always assumes that pedestrians are determined to walk to the desired (intermediate) target. The modeling of different motivations is indeed an open issue; to the best knowledge of the authors, no simulation approach that can adequately model those concepts exists. The plots for the 90-degree experiment with similar results are reported in Figure 14. The deviation in speed towards the end (after 40 sec) is even stronger compared to the 180-degree experiment. While the density in the laboratory experiment approaches zero (Figure 14 (a)), the speed drops well below 1 m/s (Figure 14 (b)). As for the 180-degree intersection experiment, video recordings indicate a lag of motivation for the last pedestrians walking through the scene. Overall, it is shown that the proposed CA reproduces the time series observed in laboratory experiments adequately, at least for situations where the pedestrians are motivated to walk and do not linger. Principally, it would be possible to modify the parameters of the CA to display a kind of “lingering” behavior; however, it is yet unclear how to quantify it.

4.3 Simulation of a Large Scenario

In the following the results of two large scenario simulations are discussed. The evacuation scenario explained by Hoogendoorn et al. (2014) has been chosen as an illustrative example. It describes an area of 50x50 m², divided into 5 vertical sections of equal size. From left to right, the first 3 sections are linked by 1 opening of 2.4 m, while the last 2 sections are linked by 2 openings of 1.2m. The setting is depicted in Figure 15.

⁶ This lag of motivation is clearly visibly in the video recordings of the experiment. The recordings are available at <http://www.math.tu-berlin.de/projekte/smdpc/>

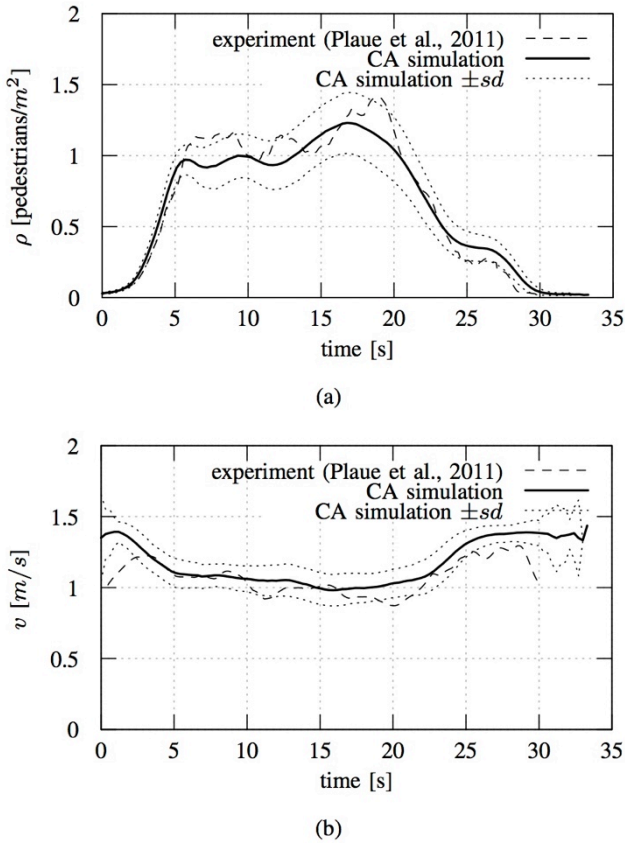


Figure 13 Time series of density and speed of 180-degree intersection experiment compared with CA simulation.

In the first experiment (top row Figure 15), a unidirectional flow similar to Hoogendoorn et al. (2014) moves through the environment from left to right. Pedestrians enter at a rate of 50 pers/s. In the second experiment, an additional flow crosses the fourth section from south to north (bottom row of Figure 15). The additional crossing-flow enters the environment at a rate of 10 pers/s. Both scenarios have been simulated with the NE route assignment approach. In iteration 1, all pedestrians follow the shortest path. This leads to congestion in front of the bottom bottleneck of the middle section. Over the iterations, this congestion dissolves. Comparing the two scenarios, the effect of the crossing flow is clearly visible. In iteration 5, congestion has almost dissolved in the unidirectional flow experiment, while in the crossing flow experiment congestion only dissolves in iteration 9. For the unidirectional experiment, the qualitative results are similar to those of Hoogendoorn (2014). The crossing flow experiment is an interesting extension, demonstrating the effect of conflicts arising from crossing flows.

4.4 Computing time analysis

A computing time analysis for the crossing flow experiment, discussed in the previous section, is shown in Figure 16 (a). It is evident that route computation never takes more

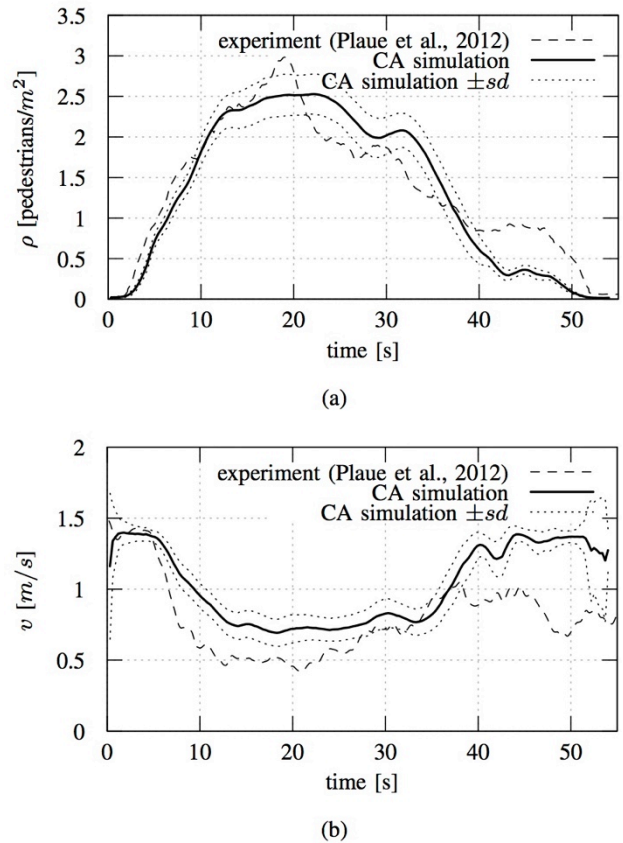


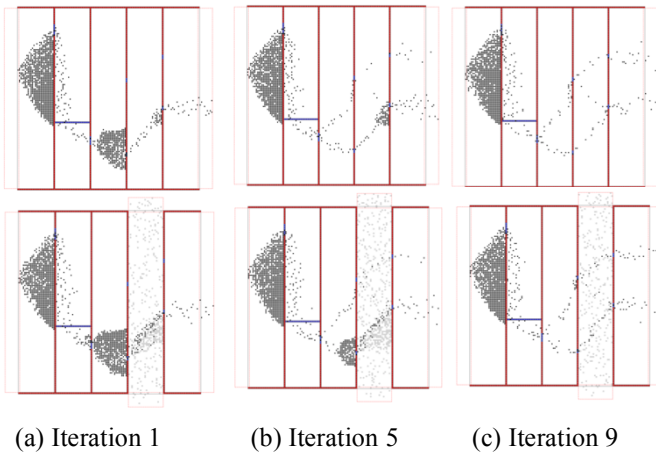
Figure 14 Time series of density and speed of 90-degree intersection experiment compared with CA simulation.

than 1 s. Moreover, the computing time for the CA simulation drops over the iterations. A reason for that is that as pedestrians find better routes, the overall congestion drops and thus the pedestrians reach their destinations earlier.

A second computing time analysis investigates the speedup of the CA simulation (i.e. the ratio of real time and computing time). Therefore, a simulation scenario consisting of a huge corridor of $80 \times 640 \text{ m}^2$ that is crossed by a total population of 50,000 pedestrians has been set up. Results of the speedup analysis are given in Figure 16 (b). It is clearly shown that the CA simulation can simulate situations with up to 13,000 pedestrians in real-time. Moreover, the computing time increases only linearly with the number of simulated pedestrians.

5 CONCLUSION AND FUTURE WORK

This contribution presented a simulation approach for multi-destination pedestrian crowds in complex environments. A novel CA simulation model induces the microscopic pedestrian dynamics. The model implements a two-dimensional representation of the environment with a square cells grid. The model reproduces empirically derived



(a) Iteration 1 (b) Iteration 5 (c) Iteration 9
Figure 15 Simulation of the large scenario: the top row unidirectional flow, bottom row crossing flow. Screenshots are taken at a same simulation time of 5:30min.

uni- and bidirectional fundamental diagrams (Zhang et al., 2011, 2012) almost perfectly.

Route assignments are achieved by an iterative approach. Depending on the cost function, the assignments move either towards a Nash equilibrium or the System optimum.

The performance of the model is tested on a set of experiments. The iterative route assignment approach is demonstrated on the well-known transport paradoxes of Braess (1968) and Daganzo (1998).

The proposed model is able to reproduce the dynamics in terms of time series of real life pedestrians stream reasonably well, demonstrated on the experimental data of

Plaue et al. (2011, 2012).

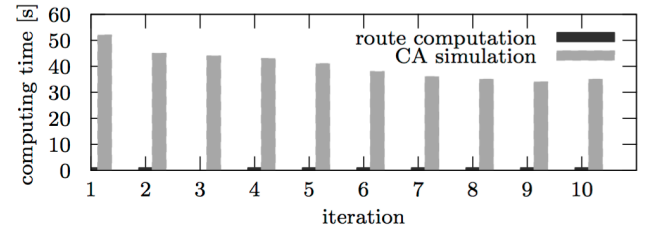
A qualitative comparison to the macroscopic large-scale evacuation scenario of Hoogendoorn (2014) finds no big differences between both simulations.

The approach simulates scenarios of the size of 10k pedestrians faster than real-time. Computing time increases only linearly with the number of simulated pedestrians, thus much larger real-time scenarios by e.g. parallelization of the CA algorithm seem to be achievable. This will be the focus of future research.

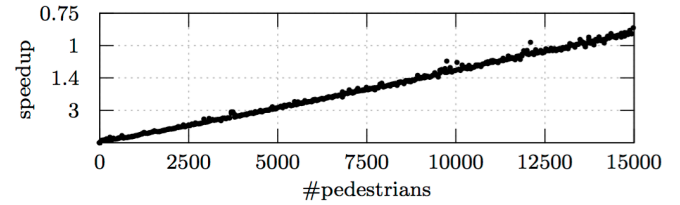
A procedure to automatically identify a configuration of the environment that moves an NE towards the SO has been sketched. The future work will implement this procedure more precisely. Another future work will be the implementation of aggregated behavior like the well-known lane formation effect in bidirectional flows. A planned technical improvement will allow for variable individual speeds. It will then also allow to simulate more complex environments like multistory buildings which include staircases and ramps.

REFERENCES

AlGadhi, S., Mahmassani, H. & Herman, R. (2002), A speed-concentration relation for bi-directional crowd movements with strong interaction. in *Pedestrian and*



(a)



(b)

Figure 16 Computing time analysis: (a) computing time of route computation and CA simulation over iteration number, (b) speedup over number of pedestrians.

Evacuation Dynamics, Springer, Berlin, Germany, pp. 3–20.

Asano, M., Iryo, T. & Kuwahara, M. (2010). Microscopic pedestrian simulation model combined with a tactical model for route choice behaviour, *Transportation Research Part C*, **18**(6), 842–855.

Baek, S., Minnhagen, P., Bernhardsson, S., Choi, K. & Kim, B. (2009), Flow improvement caused by agents who ignore traffic rules, *Physical Review E*, **80**(1), 016111.

Bandini, S., Crociani, L. & Vizzari, G. (2015), Heterogeneous pedestrian walking speed in discrete simulation models, in *Traffic and Granular Flow '13*, Springer, Berlin, Germany, pp 273–279.

Bauer, D. & Gantner, J. (2014), Including route choice models into pedestrian movement simulation models, in *Pedestrian and Evacuation Dynamics 2012*, Springer, Cham, Switzerland, pp. 713–727.

Beckmann, M., McGuire, C. & Winsten, C. (1956), *Studies in the Economics of Transportation*. Yale University Press, New Haven, CT.

Blue, V. & Adler, J. (1998), Emergent fundamental pedestrian flows from cellular automata microsimulation, *Transportation Research Record*, **1644**, 29–36.

Blue, V. & Adler, J. (2000a), Cellular automata model of emergent collective bi-directional pedestrian dynamics, in *Proceedings Artificial Life VII*, MIT Press, Cambridge, MA, USA, pp. 437–445.

Blue, V. & Adler, J. (2000b), Modeling four-directional pedestrian flows, *Transportation Research Record*, **1710**, 20–27.

Braess, D. (1968), Über ein Paradoxon aus der Verkehrsplanung, *Unternehmensforschung*, **12**, 258–268.

Burstedde, C., Klauck, K., Schadschneider, A. & Zittartz, J. (2001), Simulation of pedestrian dynamics using a two-

- dimensional cellular automaton, *Physica A*, **295**(3-4), 507–525.
- Cascetta, E. (1989), A stochastic process approach to the analysis of temporal dynamics in transportation networks, *Transportation Research Part B*, **23B**(1), 1–17.
- Charypar, D. & Nagel, K. (2005), Generating complete all-day activity plans with genetic algorithms, *Transportation*, **32**(4), 369–397.
- Chraïbi, M., Seyfried, A. & Schadschneider, A. (2010), Generalized centrifugal-force model for pedestrian dynamics. *Physical Review E*, **82**(4), 46111.
- Crociani, L., Invernizzi, A., & Vizzari, G. (2014), A hybrid agent architecture for enabling tactical level decisions in floor field approaches, *Transportation Research Procedia*, **2**, 618–623.
- Daganzo, C. (1998), Queue spillovers in transportation networks with a route choice, *Transportation Science*, **32**(1), 3–11.
- Dressler, D., Flötteröd, G., Lämmel, G., Nagel, K. & Skutella, M. (2011), Optimal evacuation solutions for large-scale scenarios, in *Operations Research Proceedings 2010*, Springer, Berlin, Germany, pp. 239–244.
- Ehtamo, H., Heliövaara, S., Korhonen, T. & Hostikka, S. (2010), Game theoretic best-response dynamics for evacuees' exit selection, *Advances in Complex Systems*, **13**(1), 113–134.
- Forcael, E., González, V., Orozco, F., Vargas, S., Pantoja, A., & Moscoso, P. (2014), Ant colony optimization model for tsunamis evacuation routes, *Computer-Aided Civil and Infrastructure Engineering*, **29**(10), 723–737.
- Flötteröd, G. & Lämmel, G. (2015), Bidirectional pedestrian fundamental diagram, *Transportation Research Part B*, **71**, 194–212.
- Fukui, M. & Ishibashi, Y. (1999), Jamming transition in cellular automaton models for pedestrians on passageway, *Journal of the Physical Society of Japan*, **68**(11), 3738–3739.
- Gawron, C. (1998), An iterative algorithm to determine the dynamic user equilibrium in a traffic simulation model, *International Journal of Modern Physics C*, **9**(3), 393–407.
- Gulikers, L., Evers, J., Muntean, A. & Lyulin, A. (2013), The effect of perception anisotropy on particle systems describing pedestrian flows in corridors. *Journal of Statistical Mechanics*, **2013**(4), P04025.
- Guo, R.-Y. & Huang, H.-J. (2011), Route choice in pedestrian evacuation: formulated using a potential field, *Journal of Statistical Mechanics*, **2011**, P04018.
- Hamacher, H.W., Heller, S., Klein, W., Köster, G. and Ruzika, S. (2011), A sandwich approach for evacuation time bounds, in *Pedestrian and Evacuation Dynamics 2010*, Springer, New York, USA, pp. 503–513.
- Helbing, D. (1998), A fluid dynamic model for the movement of pedestrians, *arXiv preprint cond-mat/9805213*.
- Helbing, D., Buzna, L., Johansson, A. & Werner, T. (2005), Self-organized pedestrian crowd dynamics: experiments, simulations and design solutions. *Transportation Science*, **39**(1), 1–24.
- Helbing, D. & Molnár, P. (1995), Social force model for pedestrian dynamics, *Physical Review E*, **51**(5), 4282.
- Henderson, L. (1971), The statistics of crowd fluids, *Nature*, **229**(5284), 381–383.
- Hoogendoorn, S. & Bovy, P. (2004a), Dynamic user-optimal assignment in continuous time and space, *Transportation Research Part B*, **38**(7), 571–592.
- Hoogendoorn, S. & Bovy, P. (2004b), Pedestrian route-choice and activity scheduling theory and models, *Transportation Research Part B*, **38**(2), 169–190.
- Hoogendoorn, S., Daamen, W., Duives, D. & Van Wageningen-Kessels, F. (2014), Optimal crowd evacuation, Annual Meeting Preprint 14-2768, Transportation Research Board, Washington D.C., USA.
- Hughes, R. (2002), A continuum theory for the flow of pedestrians. *Transportation Research Part B*, **36**(6), 507–535.
- Jiang, Y.Q., Xiong, T., Wong, S.C., Shu, C.W., Zhang, M., Zhang, P. & Lam, W.H.K. (2009), A reactive dynamic continuum user equilibrium model for bi-directional pedestrian flows, *Acta Mathematica Scientia*, **29**(6), 1541–55.
- Kemloh Wagoum, A.U., Seyfried, A. & Holl, S. (2012), Modelling dynamic route choice of pedestrians to assess the criticality of building evacuation, *Advances in Complex Systems*, **15**(07), 15.
- Kirchner, A., Nishinari, K. & Schadschneider, A. (2003), Friction effects and clogging in a cellular automaton model for pedestrian dynamics, *Physical Review E*, **67**(5), 56122.
- Kirchner, A., Klüpfel, H., Nishinari, K., Schadschneider, A. & Schreckenberg, M. (2004), Discretization effects and the influence of walking speed in cellular automata models for pedestrian dynamics, *Journal of Statistical Mechanics*, **2004**(10), P10011.
- Kretz, T., Bönsch, C. & Vortisch, P. (2010), Comparison of various methods for the calculation of the distance potential field, in *Pedestrian and Evacuation Dynamics 2008*, Springer, Berlin Heidelberg, Germany, pp. 335–346.
- Kretz, T., Grünebohm, A., Kaufman, M., Mazur, F. & Schreckenberg, M. (2006), Experimental study of pedestrian counterflow in a corridor. *Journal of Statistical Mechanics*, **2006**(10), P10001.
- Kretz, T., Lehmann, K. & Hofsäß, I. (2014), User equilibrium route assignment for microscopic pedestrian simulation, *Advances in Complex Systems*, **17**(2), 1450010.
- Lämmel, G. & Flötteröd, G. (2009), Towards system optimum: Finding optimal routing strategies in time-dependent networks for large-scale evacuation problems, in *KI 2009: Advances in Artificial Intelligence*, Vol. 5803 of *LNCS (LNAI)*, Springer, Berlin, Germany, pp. 532–539.

- Lämmel, G. & Flötteröd, G. (2015), A CA model for bi-directional pedestrian streams, *Procedia Computer Science*, **52**, 950–955.
- Lämmel, G., Klüpfel, H. & Nagel, K. (2009), The MATSim network flow model for traffic simulation adapted to large-scale emergency egress and an application to the evacuation of the Indonesian city of Padang in case of a tsunami warning, in *Pedestrian Behavior*, Emerald Publishing, Bingley, West Yorkshire, UK, pp. 245–265.
- Lämmel, G., Grether, D. & Nagel, K. (2010), The representation and implementation of time-dependent inundation in large-scale microscopic evacuation simulations. *Transportation Research Part C*, **18**(1), 84–98.
- Liu, X., Song, W. & Lv, W. (2014), Empirical data for pedestrian counterflow through bottlenecks in the channel, *Transportation Research Procedia*, **2**, 34–42.
- Metropolis, N., Rosenbluth, A., Rosenbluth, M. & Teller, A. (1953), Equation of state calculations by fast computing machines, *Journal of Chemical Physics*, **21**(6), 1087–1092.
- Michon, J. (1985), A critical view of driver behavior models: What do we know, what should we do?, in *Human Behavior and Traffic Safety*, Springer, New York, USA, pp. 485–524.
- Moussa, N. (2008), Simon-Gutowitz bidirectional traffic model revisited, *Physics Letters A*, **372**(45), 6701–6704.
- Muramatsu, M. & Nagatani, T. (2000), Jamming transition in two-dimensional pedestrian traffic, *Physica A*, **275**(1–2), 281–201.
- Muramatsu, M., Irie, T. & Nagatani, T. (1999), Jamming transition in pedestrian counter flow, *Physica A*, **267**(3–4), 487–498.
- Nagel, K., Esser, J. & Ricker, M. (2000), Large-scale traffic simulations for transportation planning. *Annual Review of Computational Physics*, **7**, 151–202.
- Nagel, K. & Schreckenberg, M. (1992), A cellular automaton model for freeway traffic, *Journal de Physique I*, **2**(12), 2221–2229.
- Nagel, K., Wolf, D., Wagner, P. & Simon, P. (1998), Two-lane traffic rules for cellular automata: A systematic approach, *Physical Review E*, **58**(2), 1425.
- Nash, J. (1951), Non-cooperative games, *The Annals of Mathematics*, **54**(2), 286–295.
- Peeta, S. & Mahmassani, H. (1995), System optimal and user equilibrium time-dependent traffic assignment in congested networks, *Annals of Operations Research*, **60**(1), 81–113.
- Plaue, M., Chen, M., Bärwolff, G. & Schwandt, H. (2011), Trajectory extraction and density analysis of intersecting pedestrian flows from video recordings, in *Proceedings of the 2011 ISPRS conference on Photogrammetric image analysis*, Vol. 6952 of LNCS, Springer, Berlin Heidelberg, Germany, pp. 285–296.
- Plaue, M., Minjie, C., Bärwolff, G. & Schwandt, H. (2012), Multi-view extraction of dynamic pedestrian density fields, *Photogrammetrie - Fernerkundung - Geoinformation*, **2012**(5), 547–555.
- Raney, B. & Nagel, K. (2004), Iterative route planning for large-scale modular transportation simulations, *Future Generation Computer Systems*, **20**(7), 1101–1118.
- Rickert, M., Nagel, K., Schreckenberg, M. & Latour, A. (1996), Two lane traffic simulations using cellular automata, *Physica A*, **231**(4), 534–550.
- Roughgarden, T. (2005), *Selfish Routing and the Price of Anarchy*. MIT Press, Cambridge, MA, USA.
- Simon, P. & Gutowitz, H. (1998), Cellular automaton model for bidirectional traffic, *Physical Review E*, **57**(2), 2441–2444.
- Steffen, B. & Seyfried, A. (2010), Methods for measuring pedestrian density, flow, speed and direction with minimal scatter, *Physica A*, **389**(9), 1902–1910.
- Sun, Q. & Wu, S. (2014), A configurable agent-based crowd model with generic behavior effect representation mechanism, *Computer-Aided Civil and Infrastructure Engineering*, **29**(7), 531–545.
- von Sivers, I. & Köster, G. (2015), Dynamic stride length adaptation according to utility and personal space, *Transportation Research Part B*, **74**, 104–117.
- Wardrop, J. (1952), Some theoretical aspects of road traffic research, *Proceedings of the Institute of Civil Engineers*, **1**, 325–378.
- Weidmann, U. (1993), Transporttechnik der Fussgänger, in *Schriftreihe des IVT*, Vol. 90, Institute for Transport Planning and Systems ETH Zurich. Zurich, Switzerland.
- Whiting, P. & Hillier, J. (1960), A method for finding the shortest route through a road network, *Operational Research Quarterly*, **11**(1), 37–40.
- Xiong, T., Zhang, M., Shu, C.W., Wong, S.C., & Zhang, P. (2011), High-Order Computational Scheme for a Dynamic Continuum Model for Bi-Directional Pedestrian Flows, *Computer-Aided Civil and Infrastructure Engineering*, **26**(4), 298–310.
- Youn, H., Gastner, M.T. & Joeng, H. (2008), Price of Anarchy in Transportation Networks: Efficiency and Optimal Control, *Physical Review Letters*, **101**, 128701.
- Youn, H., Gastner, M.T. & Joeng, H. (2009), Erratum: Price of Anarchy in Transportation Networks: Efficiency and Optimal Control [Phys. Rev. Lett. 101, 128701 (2008)], *Physical Review Letters*, **102**, 049905.
- Zhang, J., Klingsch, W., Schadschneider, A. & Seyfried, A. (2011), Transitions in pedestrian fundamental diagrams of straight corridors and t-junctions, *Journal of Statistical Mechanics*, **2011**(06), P06004.
- Zhang, J., Klingsch, W., Schadschneider, A. & Seyfried, A. (2012), Ordering in bidirectional pedestrian flows and its influence on the fundamental diagram, *Journal of Statistical Mechanics*, **2012**(02), P02002.
- Zhang, J. & Seyfried, A. (2014), Comparison of intersecting pedestrians flows based on experiments. *Physica A*, **405**, 316–325.